Molecular Biology Reports (2022) 49:2847–2856
https://doi.org/10.1007/s11033-021-07098-y

ORIGINAL ARTICLE

Modified uvsY by N-terminal hexahistidine tag addition enhances efficiency of recombinase polymerase amplification to detect SARS-CoV-2 DNA

Kevin Maafu Juma[1] · Teisuke Takita[1] · Masaya Yamagata[1] · Mika Ishitani[1] · Kaichi Hayashi[1] · Kenji Kojima[1,2] · Koichiro Suzuki[3] · Yuri Ando[4] · Wakao Fukuda[4] · Shinsuke Fujiwara[4] · Yukiko Nakura[5] · Itaru Yanagihara[5] · Kiyoshi Yasukawa[1]

Received: 20 October 2021 / Accepted: 16 December 2021 / Published online: 31 January 2022

Abstract

Background Recombinase (uvsY and uvsX) from bacteriophage T4 is a key enzyme for recombinase polymerase amplification (RPA) that amplifies a target DNA sequence at a constant temperature with a single-stranded DNA-binding protein and a strand-displacing polymerase. The present study was conducted to examine the effects of the N- and C-terminal tags of uvsY on its function in RPA to detect SARS-CoV-2 DNA.

Methods Untagged uvsY (uvsY-Δhis), N-terminal tagged uvsY (uvsY-Nhis), C-terminal tagged uvsY (uvsY-Chis), and N- and C-terminal tagged uvsY (uvsY-NChis) were expressed in *Escherichia coli* and purified. RPA reaction was carried out with the in vitro synthesized standard DNA at 41 °C. The amplified products were separated on agarose gels.

Results The minimal initial copy numbers of standard DNA from which the amplified products were observed were 6×10^5, 60, 600, and 600 copies for the RPA with uvsY-Δhis, uvsY-Nhis, uvsY-Chis, and uvsY-NChis, respectively. The minimal reaction time at which the amplified products were observed were 20, 20, 30, and 20 min for the RPA with uvsY-Δhis, uvsY-Nhis, uvsY-Chis, and uvsY-NChis, respectively. The RPA with uvsY-Nhis exhibited clearer bands than that with either of other three uvsYs.

Conclusions The reaction efficiency of RPA with uvsY-Nhis was the highest, suggesting that uvsY-Nhis is suitable for use in RPA.

Keywords Isothermal DNA amplification · Hexahistidine tag · Recombinase polymerase amplification (RPA) · uvsY

✉ Kiyoshi Yasukawa
yasukawa.kiyoshi.7v@kyoto-u.ac.jp

[1] Division of Food Science and Biotechnology, Graduate School of Agriculture, Kyoto University, Kyoto 606-8502, Japan

[2] Faculty of Pharmaceutical Sciences, Himeji Dokkyo University, Himeji, Hyogo 670-8524, Japan

[3] The Research Foundation for Microbial Diseases of Osaka University, Suita, Osaka 565-0871, Japan

[4] Department of Biosciences, School of Biological and Environmental Sciences, Kwansei-Gakuin University, Sanda, Hyogo 669-1337, Japan

[5] Department of Developmental Medicine, Research Institute, Osaka Women's and Children's Hospital, Izumi-shi, Osaka 594-1101, Japan

Abbreviations

RPA Recombinase polymerase amplification
SSB Single-stranded DNA-binding protein

Introduction

Recombinase polymerase amplification (RPA) amplifies a target DNA sequence at a constant temperature around 37–42 °C [1–3]. In RPA, recombinase (Rec) binds to the primers using its ATP hydrolysis activity. The primers of the resulting complex bind to the homologous sequence of the DNA template. Single-stranded DNA-binding protein (SSB) binds to the unwound strand. Strand-displacing DNA polymerase (Pol) extends the primer while SSB binds to the dispatched strand. In this way, a new DNA strand is synthesized. Unlike PCR that requires thermal cycling, RPA eliminates the use of specialized equipment such as

a thermal cycler. In view of this, most papers on RPA so far published have highlighted the importance of RPA in point-of-care use. Indeed, main RPA targets are pathogenic organisms. Furthermore, RPA is applicable to detect RNA including SARS-CoV-2 RNA by combining with reverse transcriptase [4–6].

Since the first report of RPA [1], T4 phage uvsX and uvsY have been used as Rec, T4 phage gp32 as SSB, and *Bacillus subtilis* (*Bst*) DNA polymerase as Pol. uvsX binds to the primers, while uvsY, originally identified as the T4 recombination mediator protein acts as the loading factor to assist uvsX to bind to the primers [7]. In earlier studies, we prepared recombinant uvsX, uvsY, and gp32 using an *Escherichia coli* expression system [8]. We also examined the effects of each component of the reaction solution on the RPA reaction efficiency and optimized the reaction conditions using a statistical method [5]. In those studies, uvsX, uvsY, and gp32 were expressed as N- and C-terminal hexahistidine-tagged (His-tagged) proteins with a thrombin recognition site. Purification was carried out from the cells by ammonium sulfate fractionation and Ni^{2+} affinity column chromatography. When treated with thrombin to cleave the His-tag, uvsY became insoluble while uvsX and gp32 remained soluble [8]. Therefore, we used untagged uvsX and gp32 and N- and C-terminal tagged uvsY to optimize reaction conditions [5]. However, it is possible that the uncleaved tag has a negative effect on the RPA reaction. In this study, we examined the effects of N- and C-terminal His-tags of uvsY on its function in RPA using SARS-CoV-2 DNA as a model target.

Materials and methods

Materials

uvsX and gp32 were expressed in *Escherichia coli*, as N- and C-terminal His-tagged proteins with a thrombin recognition site and purified from the cells, and the tags were removed by thrombin treatment as described previously [8]. The concentrations of uvsX and gp32 were determined using the molar absorption coefficient at 280 nm of 33,015 and 41,160 M^{-1} cm^{-1}, respectively. *Bst* DNA polymerase (large fragment) was purchased from New England BioLabs (Ipswich, MA). Creatine kinase was purchased from Roche (Mannheim, Germany). Reaction enzymes were purchased from Takara Bio (Kusatsu, Japan).

Construction of plasmids

Construction of pET-uvsY-NChis, previously termed pET-uvsY2, was described previously [8]. For the construction of pET-uvsY-NChis-2 (Supplementary Fig. 1), the DNA fragment was amplified from pET-uvsY-NChis using primers UvsY_N-thrombin-del_F (GGCAGCCATATGATGAGATTAGAAGATC) and UvsY_N-thrombin-del_R (GTGATGATGATGATGGCTGCTG) using 0.5 U of KOD-Plus-Neo (Toyobo, Osaka, Japan) with 35 cycles at 98 °C for 10 s and 68 °C for 5 min. The amplified fragment was phosphorylated at its 5' terminus with T7 polynucleotide kinase and self-ligated. For the construction of pET-uvsY-Nhis, the DNA fragment was amplified from pET-uvsY-NChis-2 using primers UvsY_N-His-only_F (TGAGATCCGGCTGCTAACAAAGC) and UvsY_N-His-only_R (TTTTCCAGCCTCAAATGCTCG) using 0.5 U of KOD-Plus-Neo with 35 cycles at 98 °C for 10 s and 68 °C for 5 min. The amplified fragments were purified with MagExtractor™-PCR & Gel Clean up- (Toyobo, Osaka, Japan) and phosphorylated at its 5' terminus using T7 polynucleotide kinase (Toyobo) and self-ligated using DNA ligation kit (Takara Bio). For the construction of pET-uvsY-Chis, the 168-bp DNA fragment corresponding to 161–328 of pET-22b(+) (Merck Millipore, Burlington, MA) was inserted into the *Xba*I and *Xho*I sites of pET-28a(+) (Merck Millipore). To the *Nde*I and *Xho*I sites of the resulting plasmid, the *Nde*I- and *Xho*I-digested 411-bp uvsY DNA fragment of pET-uvsY-1 (Supplementary Fig. 1), corresponding to DNA sequence 114,929–115,339 deposited in GenBank (KJ477686.1), was inserted. For the construction of pET-uvsY-Δhis, the DNA fragment was amplified from pET-uvsY-Chis using primers UvsY_N-His-only_F and UvsY_N-His-only_R with with 35 cycles at 98 °C for 10 s and 68 °C for 5 min. The amplified fragment was phosphorylated and self-ligated.

Expression of uvsY

Each of the four plasmids were transfected into *E. coli* BL21(DE3) [F^-, *ompT*, $hsdS_B$ (r_B^- m_B^-) *gal dcm* (DE3)] (Takara Bio) according to the manufacture's instruction. The overnight culture of the transformants (30 mL) was added to 300 mL of L broth containing 50 µg/mL kanamycin and incubated with shaking at 37 °C. When OD_{660} reached 0.6–0.8, the culture (300 mL) was added to 2000 mL of L broth containing 50 µg/mL kanamycin, and 2.0 mL of 0.5 M IPTG was added. Growth was continued at 30 °C for 4 h. The cells were harvested by the centrifugation of the culture at 3000×*g* for 10 min and suspended with 50 mL of 50 mM phosphate buffer (pH 7.2), 1 M NaCl, 2 mM phenylmethylsulfonyl fluoride (PMSF), and disrupted by sonication. After centrifugation at 20,000×*g* for 20 min, the supernatant was collected as the soluble fraction of the cells.

Purification of uvsY-Δhis

Solid $(NH_4)_2SO_4$ was added to the soluble fraction of the cells to a final concentration of 30% saturation. Following

the centrifugation at 20,000×*g* for 20 min, the supernatant was collected and adjusted to a final concentration of 80% saturation. Following the centrifugation, the pellet was collected and dissolved in 100 mL of buffer A (50 mM Tris-HCl (pH 8.0), 1 mM dithiothreitol (DTT)) and applied to the column packed with Toyopearl DEAE-650 M (Tosoh, Tokyo, Japan) equilibrated with buffer A. After washing with buffer A, the bound uvsY-Δhis was eluted with each 20 mL of buffer A containing 100, 200, and 300 mM NaCl. Each fraction (5 mL) was assessed for the presence of uvsY-Δhis by SDS-PAGE. The active fractions were collected, concentrated to 1 mL in 10 mM Tris-HCl (pH 8.0) by Amicon Ultra-15 MWCO 10 k (Merck Millipore, Burlington, MA), and stored in 10 mM Tris-HCl (pH 8.0), 20% v/v glycerol at −30 °C. The uvsY-Δhis concentration was determined by the method of Bradford using Protein Assay CBB Solution (Nacalai Tesque, Kyoto, Japan) with bovine serum albumin (Nacalai Tesque) as standard.

Purification of uvsY-Nhis, uvsY-Chis, and uvsY-NChis

Solid $(NH_4)_2SO_4$ was added to the soluble fraction of the cells to a final concentration of 40% saturation. In uvsY-NChis, following the centrifugation, the pellet was dissolved in 50 mL of buffer B (50 mM phosphate buffer (pH 7.2), 500 mM NaCl). In uvsY-Nhis and uvsY-Chis, following the centrifugation, the supernatant was collected and adjusted to a final concentration of 60% and 80% saturation, respectively. Following the centrifugation, the pellet was dissolved in 50 mL of buffer B. The solution was applied to the column packed with a Ni^{2+}-sepharose (Profinity IMAC resin 5 mL, BioRad, Hercules, CA) equilibrated with buffer B. After washing with 100 mL buffer B containing 100 mM imidazole, the bound enzyme was eluted with 300 mL of buffer B containing 600 mM imidazole. The active fractions were collected and concentrated as described above. The uvsY concentration was determined by the method of Bradford as described above.

Solubility test

uvsY (0.2 μg/mL in 50 mM Tris-HCl buffer (pH 8.6)) was incubated at 42 °C for specified time (10–60 min) followed by the centrifugation at 15,000×*g* for 10 min. The absorbance at 280 nm (A_{280}) of the supernatant was measured with a Jasco spectrophotometer model V-550 (Japan Spectroscopic Company, Tokyo, Japan).

RPA reaction

The RPA detection system for SARS-CoV-2 DNA was used (Supplementary Fig. 2) [5]. Unless otherwise indicated, the reaction condition was 400 ng/μL uvsX, 40 ng/μL uvsY, 400 ng/μL gp32, 0.4 units/μL *Bst* DNA polymerase, 120 ng/μL creatine kinase, 2 mM DTT, 6% PEG35000, 3.5 mM ATP, 650 mM dNTPs, 50 mM Tris-HCl buffer (pH 8.6), 40 mM CH_3COOK, 20 mM phosphocreatine, 8 mM $Mg(OCOCH_3)_2$, 1 μM 2 F-15 primer, 1 μM 2R-11 primer at 41 °C for 30 min. The reaction was performed in a 0.2 ml PCR tube in PCR Thermal Cycler Dice (Takara Bio). The amplified products were separated on 2.0% (w/v) agarose gels and stained with ethidium bromide (1 μg/ml).

Results

Design and preparation of recombinant uvsY with or without His-tag

The His-tag is known to facilitate the purification of recombinant proteins. However, it sometimes decreases the solubility and activity of proteins [9]. We previously expressed recombinant uvsX, uvsY, and gp32 as N- and C-terminal His-tagged proteins with a thrombin recognition site. In uvsX and gp32, the tags were removed by thrombin treatment. Meanwhile, thrombin treatment of the N- and C-terminal His-tagged uvsY (uvsY-NChis) resulted in precipitation [8]. Fortunately, untreated uvsY-NChis was functional in the RPA reaction [8], indicating that the His-tag of uvsY does not abolish its function in RPA. However, it is possible that the uncleaved His-tag decreases the function of uvsY. To address this issue, we designed three new forms of uvsY, i.e., untagged uvsY (uvsY-Δhis), N-terminal His-tagged uvsY (uvsY-Nhis), and C-terminal His-tagged uvsY (uvsY-Chis). Figure 1 shows the *E. coli* expression plasmids for these three uvsYs and uvsY-NChis. These four genes were expressed in *E. coli* BL21(DE3) cells.

Purification was based on the procedure we previously described [8], but with several modifications. First, polyethyleneimine treatment of the soluble fraction of the cells, which was originally included to remove nucleic acids, was excluded. This prevented the viscosity of the solution from becoming so high that the flow rate of the successive Ni^{2+} affinity column chromatography was reduced. Second, ammonium sulfate fractionation was used instead. The ammonium sulfate concentrations at which uvsY-Δhis, uvsY-Nhis, uvsY-Chis, and uvsY-NChis precipitated were 80%, 60%, 80%, and 40% saturation, respectively, indicating that the uvsY-NChis was the least soluble. In order to obtain highly purified uvsY that could be used in RPA reaction, Ni^{2+} affinity chromatography was used for uvsY with His-tag (uvsY-Nhis, uvsY-Chis, and uvsY-NChis), while anion exchange column chromatography was used for uvsY without His-tag (uvsY-Δhis). From a 2 L culture, 25, 11, 11, and 9 mg of uvsY-Δhis, uvsY-Nhis, uvsY-Chis, and uvsY-NChis were obtained.

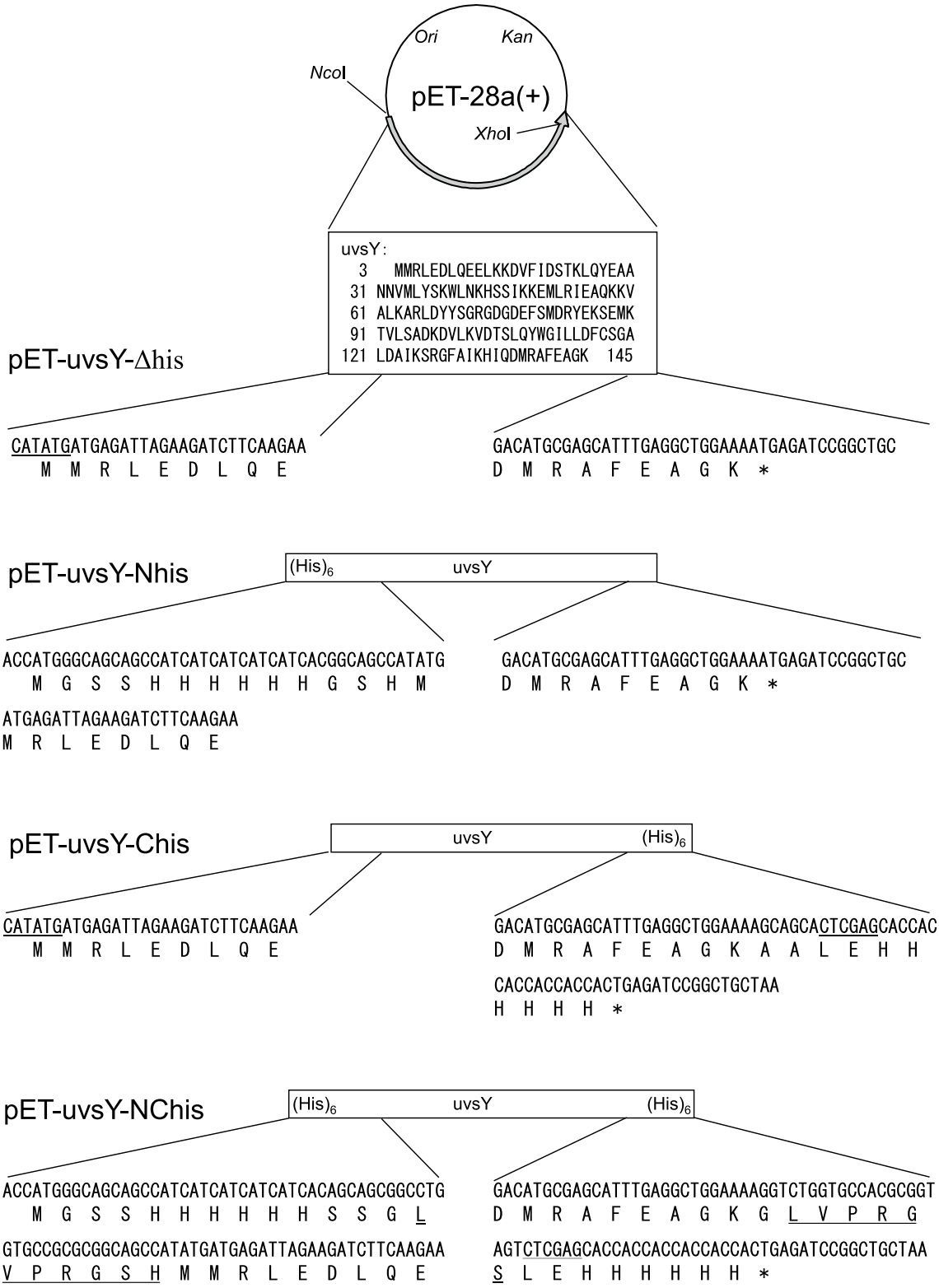

Fig. 1 Expression plasmids. The asterisk indicates the termination codon. The thrombin recognition sequence and *Nde*I and *Xho*I sites are underlined

Figure 2 shows the results of the SDS-PAGE analysis of the active fractions at each purification stage and the purified enzyme preparations. The purified uvsY-Δhis, uvsY-Nhis, uvsY-Chis, and uvsY-NChis preparations yielded single bands with molecular masses of 16, 17, 17, and 22 kDa, respectively. The molecular masses of these uvsYs calculated from the amino acid sequences were 15,952, 17,419, 17,159, and 19,847 Da, respectively (Fig. 1 and Supplementary Fig. 2), indicating that the two molecular masses were considerably different for uvsY-NChis, but were almost similar for uvsY-Δhis, uvsY-Nhis, and uvsY-Chis. These results suggested that when both the N- and C-terminal His-tags were present, the structure of uvsY was considerably altered.

Comparison of the solubility of uvsY with or without His-tag

The remaining soluble protein concentration was determined after thermal treatment at 42 °C. The natural logarithm of the soluble fraction was plotted against the incubation time (Supplementary Fig. 4). The soluble fraction of uvsY-Δhis were stable. The soluble fraction of uvsY-Nhis decreased to 15% at 60 min. The soluble fractions of uvsY-Chis and uvsY-NChis decreased more rapidly than did uvsY-Nhis, and decreased to less than 5% at 60 min. These results indicated that the solubility was in the order of uvsY-Δhis > uvsY-Nhis > uvsY-Chis ≈ uvsY-NChis, suggesting that the presence of His-tag, especially C-terminal His-tag, reduced the solubility of uvsY.

Comparison of the optimal concentration of uvsY with or without His-tag in RPA

The effect of each uvsY concentration on the RPA reaction efficiency was examined. For this purpose, the RPA detection system for SARS-CoV-2 (Supplementary Fig. 3), which we established previously [5], was used. Figure 3 shows the analysis of the products in the RPA reaction with each uvsY using agarose gel electrophoresis. The uvsY concentrations at which amplified DNA band was observed were 10–20 ng/μL for uvsY-Δhis, 10–40 ng/μL for uvsY-Nhis, 10–100 ng/μL for uvsY-Chis, and 40–100 ng/μL for uvsY-NChis. Non-specific bands were observed at 10–100 ng/μL uvsY-Δhis.

Our previous results indicated that uvsY concentrations that are too low or excessive are detrimental for the reaction [5]. These findings were also evident for uvsX, gp32, and ATP [5]. Thus, our results suggested that the specific activity of uvsY-Nhis was higher than those of the other three uvsY. We set 20, 20, 80, and 60 ng/μL as the optimal concentrations of uvsY-Δhis, uvsY-Nhis, uvsY-Chis, and uvsY-NChis, respectively, and conducted the subsequent experiments.

Comparison of sensitivity and speed of RPA reaction using uvsY with or without His-tag

For comparison of sensitivity, RPA reaction was carried out using each uvsY with $60-6\times10^7$ copies of standard DNA at 41 °C for 30 min. In the analysis of the products in the subsequent electrophoresis, the minimal initial copy numbers of standard DNA from which the amplified products were observed were 6×10^5, 60, 600, and 600 copies for the RPA with uvsY-Δhis, uvsY-Nhis, uvsY-Chis, and uvsY-NChis, respectively (Fig. 4). Several non-specific bands were observed at $0-6\times10^3$ copies for the RPA with uvsY-Δhis (lanes 1−4 in Fig. 4 A). This might be due to that uvsY-Δhis was less functional as the loading factor because Ni^{2+} affinity chromatography cannot be used for its purification, and the uvsY-Δhis preparation contained more impurities, than other three uvsY preparations.

For comparison of speed, RPA reaction was carried out using each uvsY with 6,000 copies of standard DNA at 41 °C for 10−60 min. The minimal reaction time at which the amplified products were observed were 20, 20, 30, and 20 min for the RPA with uvsY-Δhis, uvsY-Nhis, uvsY-Chis, and uvsY-NChis, respectively (Fig. 5). More importantly, the RPA with uvsY-Nhis exhibited clearer bands than that with either of other three uvsYs. These results indicated that the reaction efficiency of RPA with uvsY-Nhis was higher than that with either of the other three.

Discussion

Besides PCR and RPA, many other DNA amplification techniques have been developed. They include strand displacement amplification (SDA) [10], loop-mediated isothermal amplification (LAMP) [11], and self-assembled DNA dendrimer [12, 13]. Except for self-assembled DNA dendrimer that is an enzyme-free, the performance of a nucleic acid amplification technique depends largely on the performance of the enzymes and proteins involved. RPA uses uvsX and uvsY as Rec, gp32 as SSB, *Bst* DNA polymerase as Pol, and creatine kinase. In this study, we targeted uvsY and compared four uvsY constructions (uvsY-Δhis, uvsY-Nhis, uvsY-Chis, and uvsY-NChis) for function in RPA reaction. The results have revealed that the reaction efficiency of RPA with N-terminal tagged uvsY, uvsY-Nhis, was highest while that with untagged uvsY, uvsY-Δhis was the lowest.

It was first reported that by gel-shift assay, uvsX, uvsY, and gp32 form a ternary complex with a single-stranded DNA (ssDNA) [14]. The presence of the ternary complex was also observed using surface plasmon resonance and isothermal titration calorimetry [15]. However, binding of uvsY to ssDNA lessens the subsequent binding of the ssDNA to gp32 [15]. Thus, uvsY and gp32 bind to ssDNA

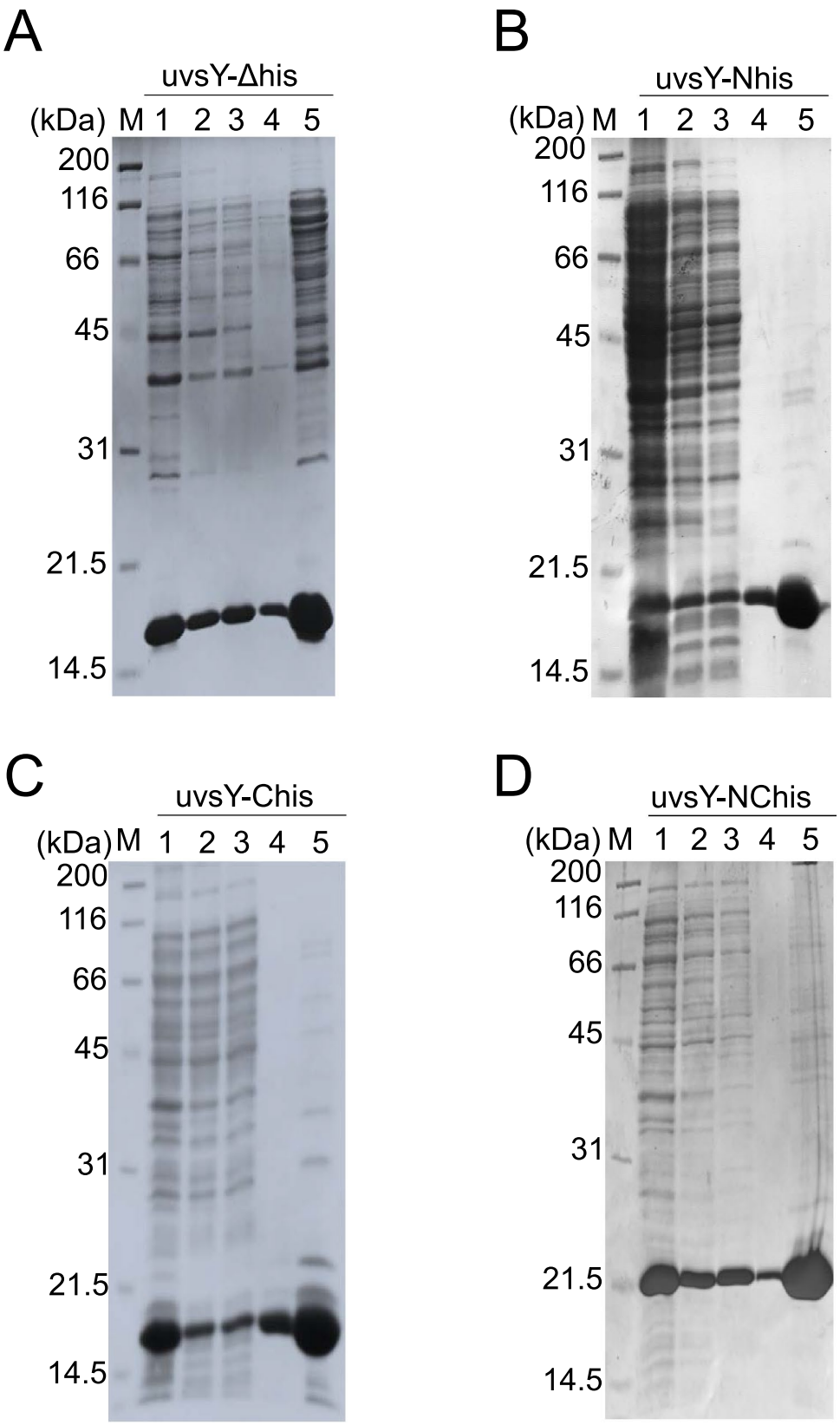

Fig. 2 Purification of uvsY. SDS-PAGE was conducted under reducing conditions. Coomassie Brilliant Blue-stained 12.5% SDS-polyacrylamide gels are shown. Marker proteins (lane M), total cell extracts (lane 1), soluble fractions of the total cell extracts (lane 2), the centrifuged pellets after fractionation by ammonium sulfate (lane 3), active fractions of anion-exchange chromatography for uvsY-Δhis (A) and Ni^{2+} affinity chromatography for uvsY-Nhis (B), uvsY-Chis (C), and uvsY-NChis (D) (lane 4), and purified preparations after membrane concentration (lane 5)

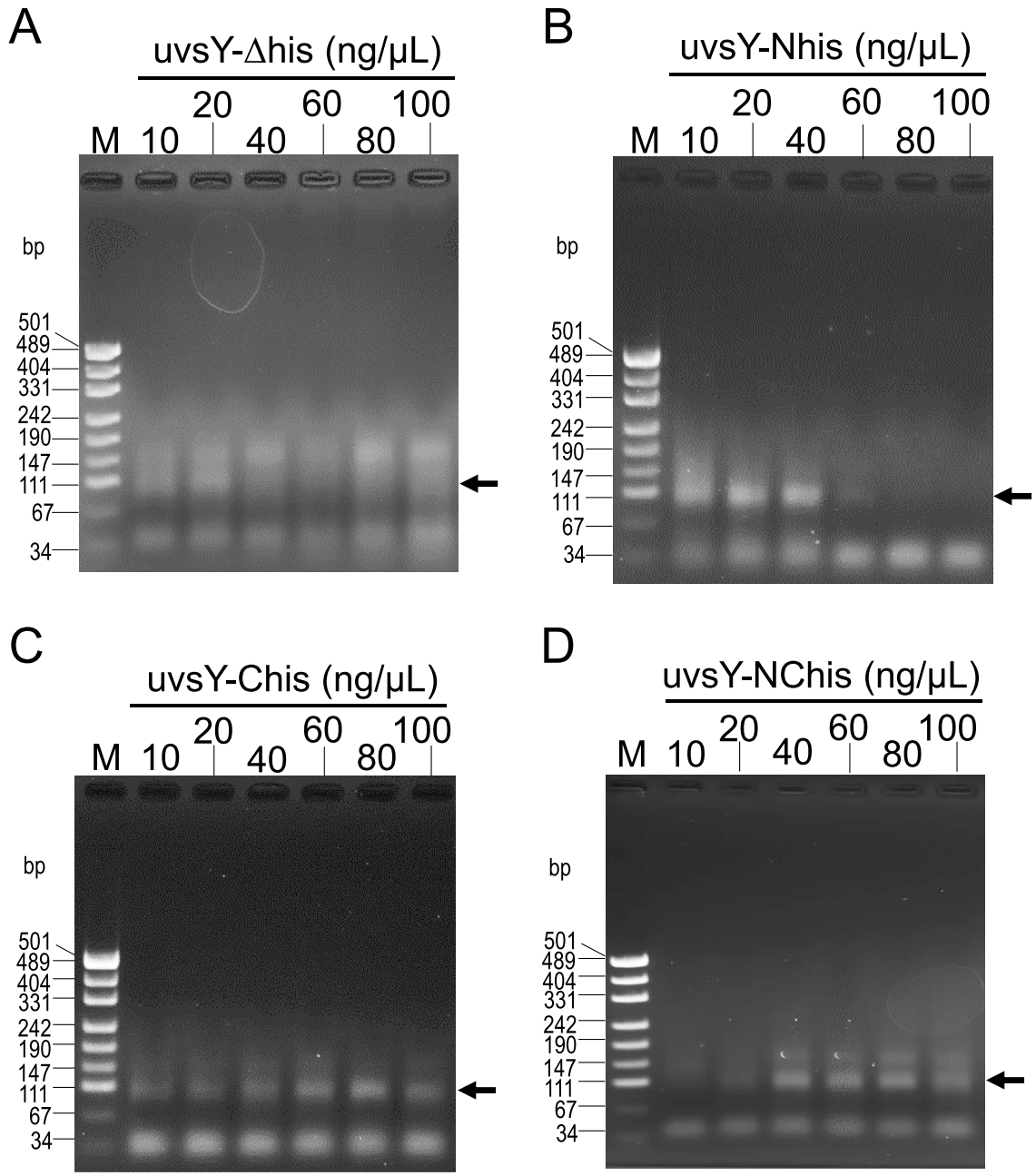

Fig. 3 Effects of the concentrations of uvsY on the reaction efficiency of RPA. The reactions were carried out with 10, 20, 40, 60, 80, and 100 ng/μL uvsY-Δhis (**A**), uvsY-Nhis (**B**), uvsY-Chis (**C**), or uvsY-NChis (**D**) at 41 °C for 30 min. Initial copies of standard DNA was 6000. The arrow indicates the 99-bp target band

competitively. In the RPA process, this competition should be adjusted to achieve a high reaction efficiency by optimizing the concentrations of uvsX, uvsY, gp32, and ATP. If the binding of uvsY to DNA primer is not strong enough, the binding of uvsX to DNA primer will also not be strong enough. Thus, the DNA primer cannot invade double-stranded DNA, preventing it from binding to the target sequence. In contrast, if the binding of uvsY to DNA primer is too strong, the binding of uvsX to the DNA primer will be also too strong, and uvsX will remain occupied even after the elongation starts. This will prevent another nucleoprotein from binding to the target sequence and initiating the elongation.

The first crystallographic analysis of uvsY reported that uvsY exists as a hexamer [16]. A more recent crystallographic analysis revealed that it exists as a heptamer and that one uvsY molecule consists of four α-helices (H1–H4: H1, E5–Y14; H2, L21–S65; H3, K80–S88; and

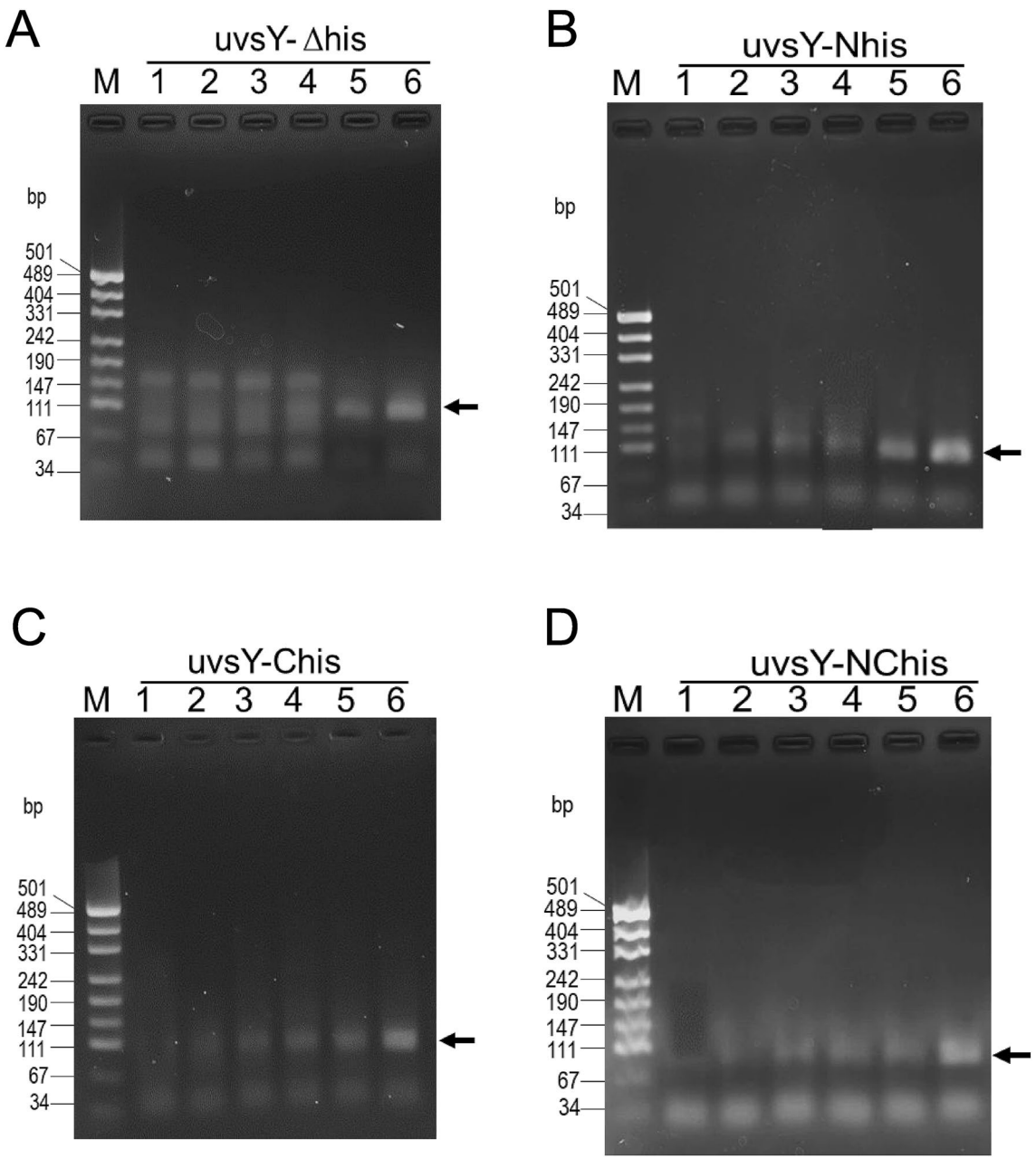

Fig. 4 Effects of initial copies on the RPA reaction. The reactions were carried out with 20 ng/μL uvsY-Δhis (**A**), 20 ng/μL uvsY-Nhis (**B**), 80 ng/μL uvsY-Chis (**C**), or 60 ng/μL uvsY-NChis (**D**) at 41 °C for 30 min. Initial copies of standard DNA: 0 (lane 1), 60 (lane 2), 600 (lane 3), 6×10^3 (lane 4), 6×10^5 (lane 5), and 6×10^7 (lane 6). The arrow indicates the 99-bp target band

H4, K91–E134) [15]. When viewed from the top of the heptamer, H4 is located inside, whereas H1, H2, and H3 are located outside. In one heptamer, seven N-terminal residues are located apart from each other and seven C-terminal residues are located close together. In this study, the presence of a C-terminal His-tag of uvsY reduced its function in RPA (Figs. 3, 4 and 5). It was previously described that cleavage of the His-tag by thrombin rendered uvsY-NChis insoluble [8]. These results might be explained as follows. In the heptameric assembly, C-terminal peptides containing His-tag and thrombin recognition sequence in close proximity to each other alter the uvsY structure unfavorably, leading to decreased activity and precipitation by thrombin treatment. The results of solubility test that uvsY-Δhis exhibited higher solubility than other three uvsYs (Supplementary Fig. 4) supports this hypothesis. As for its low activity (Figs. 3, 4 and 5), we presume that the preparation contained some impurities, such as nucleic acid, that inhibited the RPA

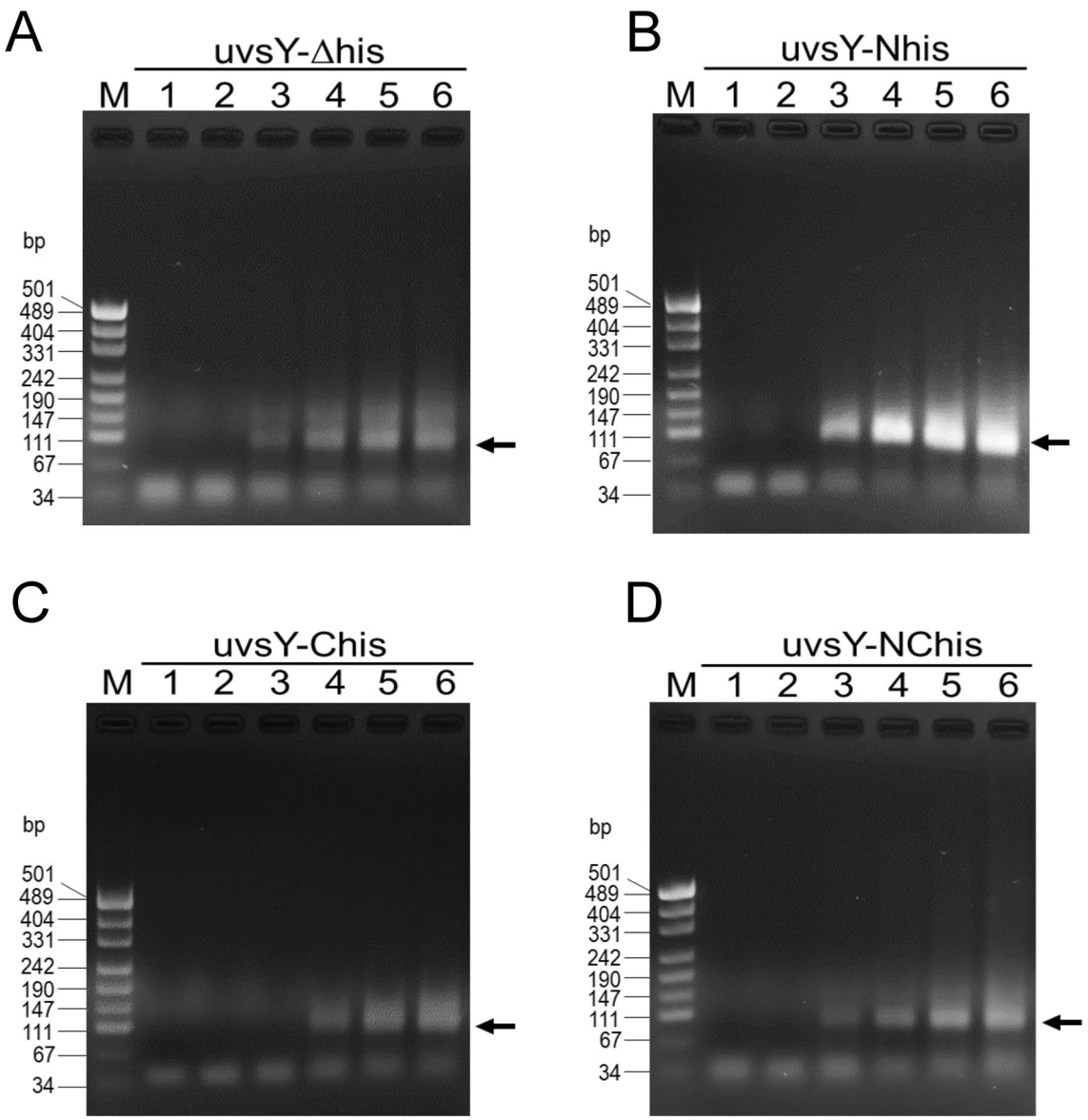

Fig. 5 Effects of reaction time on the RPA reaction. The reactions were carried out with 20 ng/μL uvsY-Δhis (**A**), 20 ng/μL uvsY-Nhis (**B**), 80 ng/μL uvsY-Chis (**C**), or 60 ng/μL uvsY-NChis (**D**) at 41 °C for 0–60 min. Initial copies of standard DNA was 6,000. Reaction time (min): 0 (lane 1), 10 (lane 2), 20 (lane 3), 30 (lane 4), 45 (lane 5), and 60 (lane 6)

reaction. Such impurities can be removed using Ni^{2+} affinity chromatography.

Conclusions

The reaction efficiency of RPA with N-terminal tagged uvsY was higher than that with untagged uvsY, C-terminal tagged uvsY, or N- and C-terminal tagged uvsY. Our results enhance the flexibility in fabricating RPA reagents for point-of-care use.

Supplementary Information The online version of this article contains supplementary material available https://doi.org/10.1007/s11033-021-07098-y.

Acknowledgements We acknowledge Mr. Kenji Ito for his technical assistance.

Author contributions KMJ, TT, and KY designed the research; KMJ, TT, MY, MI, KH, KK, YA and YN performed the research; KMJ, TT, KK, KS, WF, SF, YN, IY, and KY analyzed data; KMJ and KY wrote the manuscript.

Funding This work was supported in part by Grants-in-Aid for Scientific Research (no. 18KK0285 for T.T., K.K., and K.Y.) from Japan

Society for the Promotion of Science, Emerging/re-emerging infectious disease project of Japan (grant no. 20he0622020h0001 for S.F., I.Y., K.Y. and grant no. 20fk0108143h001 for S.F., I.Y., K.Y.) from Japan Agency for Medical Research and Development, and A-Step (no. JPMJTR20UU for K.Y.) from Japan Science and Technology Agency.

Data availability All data are available in case of need.

Declarations

Consent for publication All authors agree for publication.

Conflict of interest Authors declare that they have no conflict of interests.

Research involved in human or animal rights No experiment was conducted on animals in this study.

References

1. Piepenburg O, Williams CH, Stemple DL, Armes NA (2006) DNA detection using recombination proteins. PLoS Biol 4:e204
2. Lobato IM, O'Sullivan CK (2018) Recombinase polymerase amplification: Basics, applications and recent advances. Trends Analyt Chem 98:19–35
3. Li J, Macdonald J, von Stetten F (2019) Review: a comprehensive summary of a decade development of the recombinase polymerase amplification. Analyst 144:31–67
4. Wu T, Ge Y, Zhao K, Zhu X, Chen Y, Wu B, Zhu F, Zhu B, Cui L (2020) A reverse-transcription recombinase-aided amplification assay for the rapid detection of N gene of severe acute respiratory syndrome coronavirus 2 (SARS-CoV-2). Viroloy 549:1–4
5. Juma KM, Takita T, Ito K, Yamagata M, Akagi S, Arikawa E, Kojima K, Biyani M, Fujiwara S, Nakura Y, Yanagihara I, Yasukawa K (2021) Optimization of reaction condition of recombinase polymerase amplification to detect SARS-CoV-2 DNA and RNA using a statistical method. Biochem Biophys Res Commun 56:195–200
6. Lau YL, Ismail IB, Mustapa NIB, Lai MY, Tuan Soh TS, Haji Hassan A, Peariasamy KM, Lee YL, Abdul Kahar MKB, Chong J, Goh PP (2021) Development of a reverse transcription recombinase polymerase amplification assay for rapid and direct visual detection of Severe Acute Respiratory Syndrome Coronavirus 2 (SARS-CoV-2). PLoS ONE 16:e0245164
7. Bleuit JS, Xu H, Ma Y, Wang T, Liu J, Morrical SW (2001) Mediator proteins orchestrate enzyme-ssDNA assembly during T4 recombination-dependent DNA replication and repair. Proc Natl Acad Sci USA 98:8298–8305
8. Kojima K, Juma KM, Akagi S, Hayashi T, Takita T, O'Sullivan CK, Fujiwara S, Nakura Y, Yanagihara I, Yasukawa K (2021) Solvent engineering studies on recombinase polymerase amplification. J Biosci Bioeng 131:219–224
9. Terpe K (2003) Overview of tag protein fusions: from molecular and biochemical fundamentals to commercial systems. Appl Microbiol Biotechnol 60:523–533
10. Walker GT, Fraiser MS, Schram JL, Little MC, Nadeau JG, Malinowski DP (1992) Strand displacement amplification-an isothermal, *in vitro* DNA amplification technique. Nucleic Acids Res 20:1691–1696
11. Notomi T, Okayama H, Masubuchi H, Yonekawa T, Watanabe K, Amino N, Hase T (2000) Loop-mediated isothermal amplification of DNA. Nucleic Acids Res 28:e63
12. Yue S, Song X, Song W, Bi S (2019) An enzyme-free molecular catalytic device: dynamically self-assembled DNA dendrimers for in situ imaging of microRNAs in live cells. Chem Sci 10:1651–1658
13. Jiang Q, Yue S, Yu K, Tian T, Zhang J, Chu H, Cui Z, Bi S (2021) Endogenous microRNA triggered enzyme-free DNA logic self-assembly for amplified bioimaging and enhanced gene therapy via in situ generation of siRNAs. J Nanobiotechnol 19:288
14. Hashimoto K, Yonesaki T (1991) The characterization of a complex of three bacteriophage T4 recombination proteins, uvsX protein, uvsY protein, and gene 32 protein, on single-stranded DNA. J Biol Chem 266:4883–4888
15. Gajewski S, Waddell MB, Vaithiyalingam S, Nourse A, Li Z, Woetzel N, Alexander N, Meiler J, White SW (2016) Structure and mechanism of the phage T4 recombination mediator protein UvsY. Proc Natl Acad Sci USA 113:3275–3280
16. Xu H, Beernink HTH, Rould MA, Morrical SW (2006) Crystallization and preliminary X-ray analysis of bacteriophage T4 UvsY recombination mediator protein. Acta Crystallogr Sect F 62:1013–1015